



Application of the GIS methods along with measured parameters to identify the NH_4^+ origin in the Hranice Karst (Czech Republic)

Milan Geršl¹ · Jozef Sedláček² · Petra Oppeltová¹ · Ondřej Ulrich¹ · Kristýna Kohoutková² · Vítězslav Vlček¹ · Radim Klepárník² · Vladimír Babák³

Received: 29 April 2024 / Accepted: 24 October 2024
© The Author(s) 2024

Abstract

The study aims to determine the source of NH_4^+ ions in the mineral waters of the Hranice Karst. The study area is located in the eastern part of the Czech Republic, Europe. The area is known mainly for its carbon dioxide of deep origin; the gas was the factor that enabled the formation of hypogene karst, in the Palaeozoic limestones, as well as warm mineral waters. The limestones of the area are covered by Neogene (Miocene) sediments of variable thickness and lithology. Recurrent sampling was done at 36 sites. A total of 96 surface water samples, 65 borehole water samples and 96 karst water samples were assessed. Major anions, cations and the content of nitrogen and its forms were determined for all water samples. The soil types were characterised by a field pedological survey. The normalised difference vegetation index was calculated in QGIS and vegetation vitality was evaluated. Since places with remarkably low vegetation index were found to be linked to the occurrence of Miocene sandstones, they represent points of rather fast entry of rainwater into the ground. As the presence of carbon dioxide creates an anoxic setting underground, the entering nitrates are transformed into NH_4^+ ions. This mechanism of transformation within the nitrogen cycle explains the presence of NH_4^+ ions in areas with elevated CO_2 .

Keywords Anoxia · Nitrogen · NDVI · Hypogene karst · Hranice abyss · Mineral water

Introduction

Water pollution caused by nutrients, such as nitrogen, is a worldwide concern. Excessive nutrient content can impact aquatic environments and may result in public health risks in the case of drinking water contamination (Zhang et al. 2015, 2021; Van Meter et al. 2017). White et al. (2013) studied the effects of land use composition on nitrate levels in groundwater, suggesting a high correlation between nitrate concentrations in drinking water and agricultural land use. In addition, nitrates, along with dissolved organic carbon

(DOC), can serve as valuable indicators when determining the specific origin of water (Lorette et al. 2022).

Non-point agricultural pollution associated with agricultural activity represents a significant portion of contamination sources. Nitrogen application has been employed in agricultural concepts for decades, and quantities exceeding the requirements for plant growth have occasionally been used (Buvaneshwari et al. 2017; Lorette et al. 2022; Cui et al. 2013), resulting in the deterioration of aquatic ecosystems and beyond them. Natural hydrological and biogeochemical time shifts of water quality changes can confuse understanding when implementing conservation policies (Chen et al. 2024; Nietch et al. 2024; Bouraoui and Grizzetti 2014; Van Meter et al. 2016). Accordingly, groundwater pollution by agrochemicals, such as fertilisers, can cause complex issues of biogeochemical transformation in groundwater-dependent ecosystems (Kalvāns et al. 2021).

The ions present at the site of infiltration usually reveal the origin of the waters using GIS methods as does their relationship to the rocks found there (Maurya et al. 2023; Yadav et al. 2018). Various studies confirm the dominance

✉ Milan Geršl
milan.gersl@mendelu.cz

¹ Faculty of AgriSciences, Mendel University in Brno, Zemědělská 1665/1, Brno 613 00, Czech Republic

² Faculty of Horticulture, Mendel University in Brno, Valtická 337, Lednice 69144, Czech Republic

³ Veterinary Research Institute, Hudcova 296/70, Brno 621 00, Czech Republic

of physical processes over biogeochemical processes in transforming and gradually releasing nitrogen (Lorette et al. 2020). Spatial heterogeneity of land use and land cover is crucial in preserving a watershed (Liu et al. 2020). The impact of landscape composition (the type and proportion of land cover) and configuration (the spatial arrangement of cover types) on groundwater is often poorly understood and remains unclear. However, studies show that grassland and cropland percentages correlate with groundwater quality (Qiu and Turner 2015). Holistic vegetation research based on comprehensive monitoring was previously recommended for research on karst areas, including their spatial changes and damage (Vilhar et al. 2022). In the context of karst hydrology, land use change considerations are also promoted (Sivelle et al. 2022).

Karst aquifers, which are water sources on a global scale, exhibit a notable degree of vulnerability. The potential contribution to water supply for approximately a quarter of the global population highlights the significance of such aquifers (Ford and Williams 2007; Coxon 2011). Karst groundwater is more susceptible to pollution than water in non-karstic aquifers; the earlier also shows a significantly higher momentum of the pollutant dynamics. New multidisciplinary approaches enable the localisation of water penetrating the karst environment and a more efficient assessment of the vulnerability of karst aquifers (Sing et al. eds; Barry et al. 2023; Jiang et al. 2015; Shelar et al. 2023).

The mineral waters of the Hranice Karst have been used for therapy in the local spa resort intensely since at least 1580. Nevertheless, the places of infiltration of the waters from which these mineral waters originate are not yet known (Sracek et al. 2019). The direction of the flow of these waters is also unknown, while several large water infrastructures exist in the vicinity that supply the region with fresh water (e.g. Hao et al. 2023; Li et al. 2023; Ravbar et al. 2021), it can be assumed to take place in the Hranice Karst area as well. For this reason, we consider it essential to have possible interpretations regarding the place of groundwater seepage and the further fate of the groundwater. Numerous studies and technical papers exist that discuss the area of the Hranice Karst; however, the authors did not address the issue of possible contamination entering the waters of the deep circulation system (Sracek et al. 2019; Vysoká et al. 2019; Pavlik et al. 2018), generally assuming a zero load on the karst. The present paper aimed to determine whether or not deep karst groundwater is affected in the landscape featuring intense agricultural use and define possible sites of water infiltration as applicable. The study employs a multidisciplinary approach that includes a combination of established water analysis methods complemented by an advanced land use analysis using GIS tools.

Study area

Geological setting

The Hranice Karst (HK) is situated in the eastern region of the Czech Republic (N 49°31', E 17°45'), covering an area of approx. 15 km² at the line of contact between the eastern Bohemian Massif and the External Western Carpathians and is classified as a hypogene karst (Figs. 1 and 2). The deeper bedrock layer of the HK is made up of crystalline rocks of the Brunovistulian Unit (Precambrian). The karst territory was formed in Middle Devonian (Eifelian) to Mississippian (Viséan) carbonate rocks that were deposited on carbonate platforms and reef slopes in a tropical ocean (Macoča and Líšň Fms.). The exact thickness of the carbonate rocks is not known directly in the studied area; however, in the Choryně-9 well located 11.5 km away towards SE, approx. 1200 m of these rocks located on the crystalline bedrock were verified. In the adjacent areas, tectonically multiplied Devonian and Carboniferous strata are documented; they originated from the Variscan orogeny and are up to 7 km thick (Cháb 2010; Hladil et al. 2003; Schulmann and Gayer 2000). It is assumed that uplift and erosion occurred from the late Carboniferous to the Miocene (Jirman et al. 2018). During this long period, extensive weathering occurred and distinct karst morphology developed. The presence of mogotes and rift valleys is documented from geophysical surveying in the vicinity of Hranice (Dleštík and Bábek 2013; Tyráček 1962). The adjacent Carpathian foredeep formed during the early Miocene (Burdigalian). Subsequently, in the Miocene (early Langhian) period, there was flooding and sedimentation, both resulting in the surface of the karst relief being buried by clastic sediments, in which poorly permeable marine clays alternate with layers of more permeable conglomerates with sandstones (Sracek et al. 2019; Holcová et al. 2015). The overthrust of the West Carpathian nappes terminated the Miocene sedimentation. The current surface of the karst area consists of Quaternary loess and colluvium deposits (Supplementary Fig. 1).

The karstification of the HK took place in several stages. Carbonates were first exposed to the process at the Devonian in the Frasnian/Famenn transition. The next stages of karstification took place in the early Permian through the early Late Cretaceous and in the tropical setting of the Cretaceous period (Otava et al. 2009). Karstification took place in the Miocene as well when cockpit-like karst morphology was formed on the limestone surface and subsequently karst objects were partially filled with marine clastic sediments of the Miocene transgression (Tyráček 1962; Klanica et al. 2020). The last karstification stage is related to the emergence of carbon dioxide as mineral waters began to form during the middle Miocene regression following partial

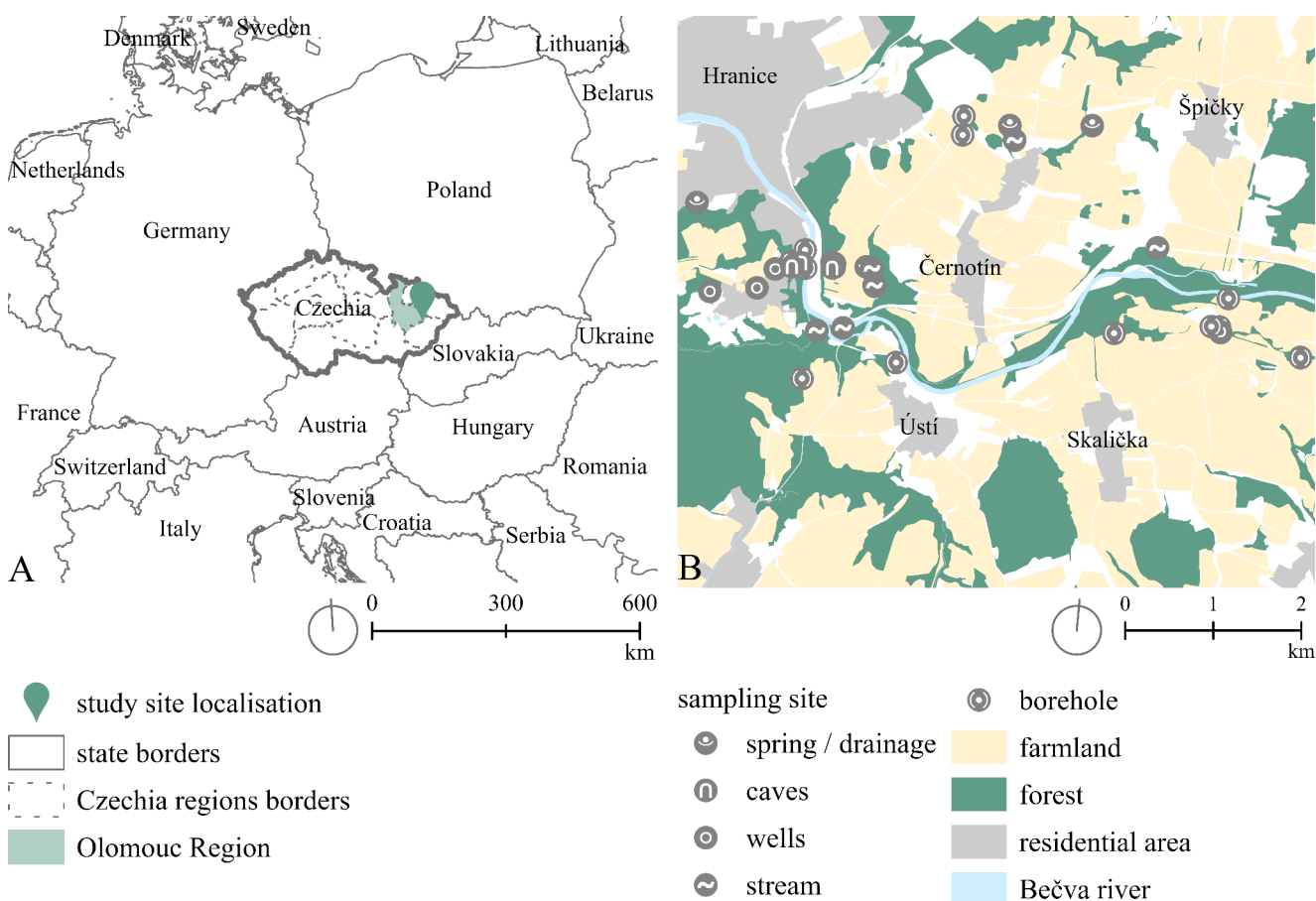


Fig. 1 A) Location of the Hranice Karst in the Czech Republic, B) Location of the sampling sites

denudation of the marine deposit from the HK surface and continues through to the present. The contact between the Bohemian Massif and the External Western Carpathians has influenced the overall tectonic structure of the HK. This younger Alpine Orogeny compression was partially reactivated via the Palaeozoic NW-SE faults that caused groundwater to circulate intensely and gas to emerge. Isotopic compositions of CO₂, combined with the ³He to ⁴He ratio, suggest that the gases originate near the Earth’s mantle transition zone (Meyberg and Rinne 1995; Šmejkal et al. 1974). Due to these processes, the hypogenic karst is considered to be the result of these events (Sracek et al. 2019; Vysoká et al. 2019; Bosák 2000) as stated by e.g. Klimchouk et al. (2017).

Climate and precipitation

In the study area, the climate is nearing the continental type. It is a moderately warm area with long, warm and moderately dry to dry summers; the transition period is short, characterised by moderately warm to warm spring and autumn seasons. Winter is short, moderately warm and very dry (Quitt 1971, 1975). According to the meteorological

analysis (Thiessen Polygon Method), which was based on the data sourced between 1961 and 2021 from hydrometeorological stations (Bělotín, Hranice, Kelč and Valašské Meziříčí) operated by the Czech Hydrometeorological Institute (CHMI), the mean annual air temperature and precipitation within the study area are 8.5 °C and 677 mm, respectively. Annual precipitation days average 150–170. There are 50–70 days with snowfall and 50–60 days with snow cover per annum (Tolasz et al. 2007). The River Bečva and its tributaries drain the whole study site (Supplementary Fig. 2a, b). In the Teplice nad Bečvou municipality, the gauge is managed by CHMI with a contributing basin area of 1275.32 km². According to CHMI, the average annual flow of the River Bečva is 14.8 m³.s⁻¹ and the average water level is 0.89 m.

Agricultural land in the Hranice Karst has an artificial drainage system installed in the 1960s (Supplementary Fig. 3). It is a special ceramic, non-perforated pipe that was buried in the ground at a depth of not more than 0.8 m. The system was supposed to drain a wetland featuring silty and clayey soils where the causes of waterlogging were complex and difficult to identify (Kulhavý et al. 2007). The

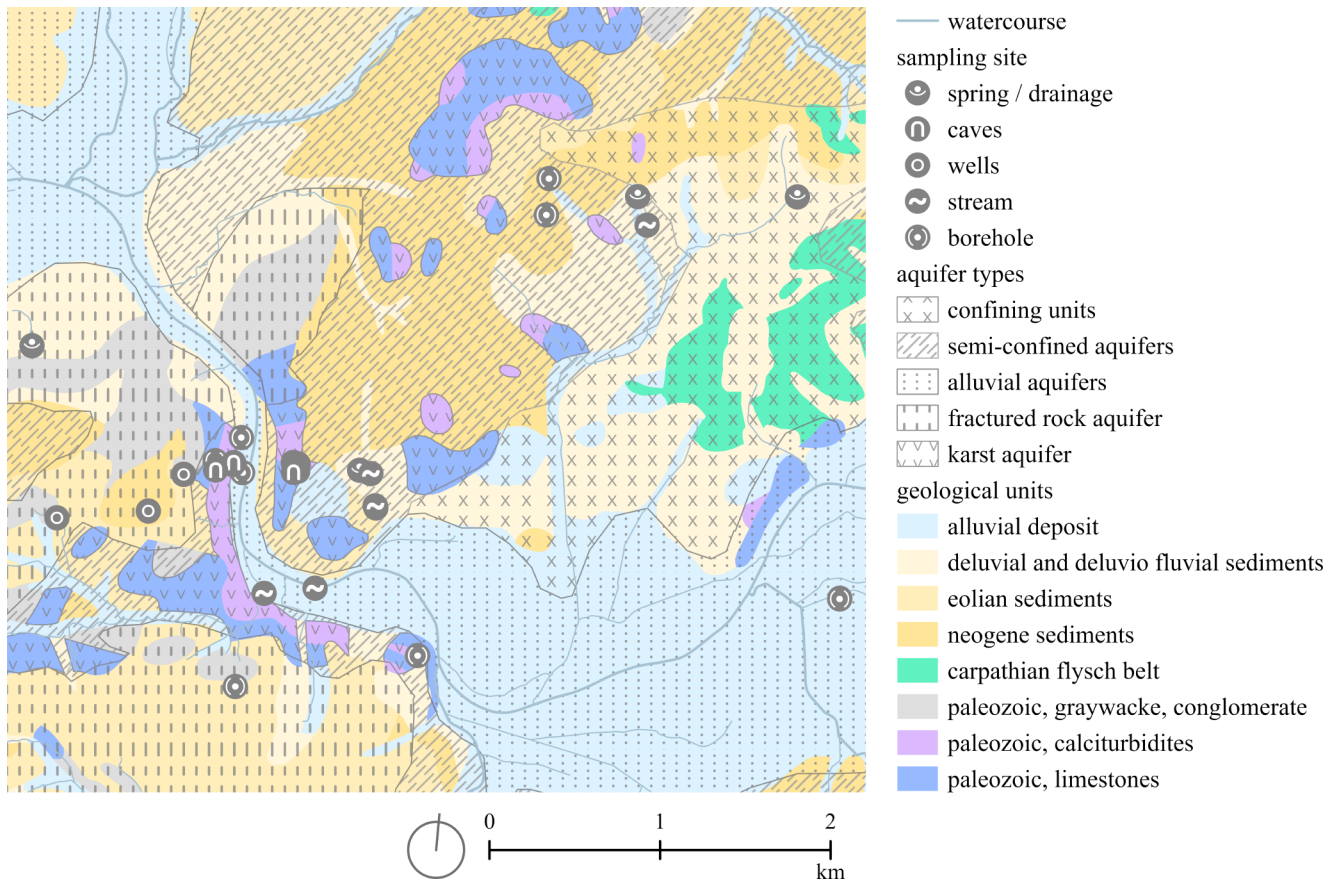


Fig. 2 Geological and hydrogeological situation (map base: Czech Geological Survey, 2004, 2018. G. Masaryk Water Research Institute, 2006)

water drained from agricultural land is discharged into surface watercourses.

Hydrogeology

Two Quaternary and Devonian groundwater aquifers are defined in the area. The Quaternary aquifer (aquifer system I) formed by the fluvial sediment of the River Bečva consists of gravels, sandy–clayish soils and relics of Pleistocene gravel river terraces. The transmissivity coefficient ranges between $1 \cdot 10^{-6}$ and $1 \cdot 10^{-4} \text{ m}^2 \cdot \text{s}^{-1}$. The general direction of groundwater flow is to the northwest, i.e. in the same direction as the River Bečva flow.

The karst aquifer (aquifer system II) is situated in Palaeozoic limestones with heterogeneous fissure–karst permeability. The transmissivity coefficient in Devonian limestones is 10^{-4} up to $1 \cdot 10^{-5} \text{ m}^2 \cdot \text{s}^{-1}$ (Řezníček 1977). Karst water emerges in the Hranice Abyss in the Zbrašov Aragonite Caves system and is pumped from deep boreholes for use by the spa resort. In the Hranice abyss, warm outflows of mineral water have been identified at depths of 30 m, 40 m, and 60 m. In the Zbrašov Aragonite Caves (ZAC) system there are lakes with mineral water in the Cave of Death

(ZAC–CD) and Lake B (ZAC–B). A layer of carbon dioxide is present above the open water surface at the sites listed above. The spa resort that utilizes CO_2 –enriched thermal water was mentioned before 1553 (Geršl 2009). New boreholes RI, RII and RIII were drilled to supply mineral water in the 20th century. As evaluated using tritium, the mean residence time of groundwater in karst aquifers in borehole RI spanned several years with comparable results. According to Švajner (1982), the residence time is 17–18 years; according to Maník et al. (1992), it is less than 42 years (9 ± 5 TU); and according to Sracek et al. (2019), it ranges between 20 and 50 years. The groundwater in the karst aquifer is of meteoric origin, with a recharge area found in the uplands situated about 200 m above the River Bečva valley (Sracek et al. 2019). For the Hranice abyss, the mean residence time was determined, using tritium and CFC, to be around 300 years (Vysoká 2016).

Methods

Fieldwork and sampling strategy

The sampling aimed at taking samples of water from surface streams, hydrogeological wells and karst waters of the area. As no apparent ponors have developed in the karst region, the sampling also covers the area of expected infiltration to the karst aquifer (Figs. 1 and 2).

The conceptual model assumes that water with nitrates enters the karst area and moves in an anaerobic environment.

Remote sensing methods and the geology of the area were used to identify the points of entry.

The water samples subjected to analysis were divided, based on the sampling site, into three groups – surface water, groundwater and karst waters (Table 1). Recurrent sampling was done at 36 sites. A total of 96 surface water samples, 65 borehole water samples and 96 karst water samples were assessed.

The Surface and shallow water group comprises the River Bečva – the primary watercourse in the area – and 96 tributaries (Tab. C); in addition, drainage water and shallow

Table 1 List of sampled sites

ID	Name/Type	WGS (La)	WGS (Lo)	Stratigraphy/Lithology	
Group 1 Surface and shallow water					
S-01	River Bečva	49.5261822	17.75412	Q, gr, sa	
S-02	Krkavec Stream	49.5254226	17.74878	Q, gr, sa	
S-03	Hluzovský Stream	49.5466135	17.77692	Q, gr, sa	
S-04	Hůrka Stream	49.5370173	17.80080	Q, gr, sa	
S-05	Vrchoviny Hill	49.5322338	17.75650	Q, cl, sa	
S-06	Vrchoviny Waterfall	49.5305455	17.75711	Q, cl, sa	
S-07	Kamenec Stream	49.5289897	17.81188	Q, cl, sa	
S-08	Hluzov Drainage	49.5480600	17.77596	Q, M, sa	
S-09	Javorová Spring	49.5372863	17.72820	Q, gr	
S-10	Hůrka Hill	49.5488215	17.78884	Q, M, sa	
S-11	Vrchoviny Drainage	49.5323509	17.75556	Q, M, cl, sa	
S-12	Vrchoviny Stream	49.5305570	17.75708	Q, M, cl, sa	
Group 2 Groundwater					
G-01	Well	49.5466571	17.76872	M, cl	
G-02	Borehole LV-56	49.5485789	17.76866	M, cl	
G-03	Well	49.5291811	17.73882	Q, M, cl	
G-04	Well	49.5283759	17.73150	Q, M, cl, sa	
G-05	Well	49.5312744	17.74140	Q, M, cl, sa	
G-06	Borehole	49.5279279	17.79524	Q, M, cl, sa	
G-07	Well	49.5290890	17.81179	Q, M, cl, sa	
G-08	Borehole	49.5271844	17.82472	Q, M, cl, sa	
G-09	Borehole HV-301	49.5358827	17.74096	P, gw	
G-10	Borehole HJ-02	49.5304493	17.75715	M, cl, sa	
G-11	Borehole	49.5229036	17.76163	P, ca.	
G-12	Borehole	49.5295541	17.81160	P, ca.	
G-13	Borehole	49.5272186	17.82467	M, cl, P, ca.	
Group 3 3a) Karst water 3b) Hypogenic karst water					
Hranice abys (HA)					
3a	HA-SWCh 6	Southwest Channel	49.5319191	17.75025	P, ca.
3b	HA-NWCh 30	Northwest Channel	49.5324326	17.75015	P, ca.
3b	HA-TS 30	Thermal Spring	49.5323726	17.75056	P, ca.
3b	HA-TS 40	Thermal Spring	49.5322292	17.75056	P, ca.
3b	HA-TS 60	Thermal Spring	49.5319970	17.75058	P, ca.
Zbrašov aragonite caves (ZAC)					
3b	ZAC-B	B Cave	49.5320245	17.74530	P, ca.
3a	ZAC-CD	Cave of Death	49.5316544	17.74395	P, ca.
3a	ZAC-NN	Nameless Cave	49.5321378	17.74536	P, ca.
Spa well					
3b	R-I	Borehole	49.5316529	17.74615	P, ca.
3b	R-II	Borehole	49.5334889	17.74578	P, ca.
3b	R-III	Borehole	49.5321471	17.74384	P, ca.

Stratigraphy: Q – Quaternary, M – Miocene, P – Palaeozoic

Lithology: ca. – carbonates, cl – clay/claystone, gr – gravel, gw – greywacke, sa – sand/sandstone

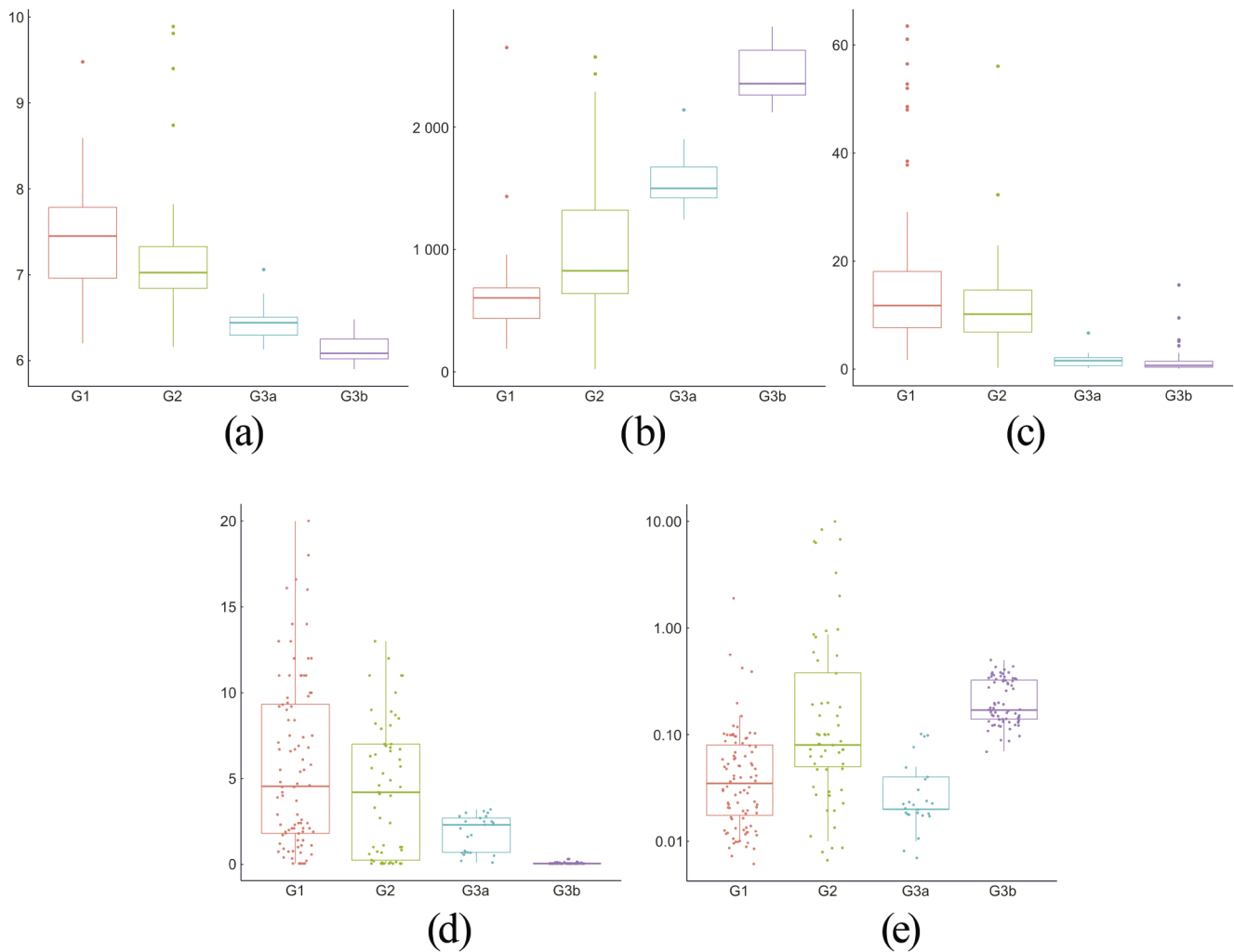


Fig. 3 a) Box plot diagram, pH; b) Box plot diagram, EC [$\mu\text{S}\cdot\text{cm}^{-1}$]; c) Box plot diagram, COD [$\text{mg}\cdot\text{l}^{-1}$]; d) Box plot diagram, $\text{N}\text{-NO}_3$ [$\text{mg}\cdot\text{l}^{-1}$]; e) Box plot diagram, $\log \text{N}\text{-NH}_4^+$ [$\text{mg}\cdot\text{l}^{-1}$]

springs belong to this group. The group of waters labelled as Groundwater was sampled from boreholes with perforated lining tubes installed, the depths ranging from 30 to 150 m. The boreholes reached Miocene clays, sandstones and Palaeozoic limestones, as well as a combination of the three types. The group identified as Karst water was collected from the Hranice abyss, the Zbrašov Aragonite Caves and the boreholes that supply water to the spa resort (Supplementary Figs. 4, 5 and 6).

Sampling and hydrochemistry analyses

Water samples were collected in 2021–2023; sampling was done every two months. The sampling was not always possible in some locations due to low water levels. The samples intended for cation and trace element analyses were pre-filtered using 0.45 μm Millipore filters and then stored in HDPE bottles for further analysis. In the Hranice Abyss,

water sampling was conducted by cave divers – members of the Czech Speleological Society.

Measurements of pH, electrical conductivity (EC) and oxidation-reduction potential (ORP) of the sampled water were performed directly in the field. Greisinger GMH 5530 with GE 117 electrode (pH), Greisinger GMH 5400 with LF 425 electrode (EC) and Greisinger GMH 5530 with GR 105 electrode (ORP) were the instruments used for the measurements.

The contents of chlorides and sulphides were analysed by an ion liquid chromatograph (Dionex ICS–2000), with a measurement uncertainty of 10%. The concentration of bicarbonate ions was analysed by the potentiometric method at pH 4.5 and 8.3 with 5% measurement uncertainty. The calcium, magnesium, sodium and potassium contents were analysed using Electromultiplier ICP–MS Agilent Technologies 7700 with a measurement uncertainty of 10%. The contents of ammonium cations and nitrate anions were

analysed using Agilent Technologies 7700 Electromultiplier ICP–MS with a measurement uncertainty of 10%. The Total nitrogen content was analysed by combustion in an O₂ atmosphere and subsequent catalytic oxidation to nitrogen oxide using TOC–Vcph Shimadzu with a measurement uncertainty of 10%. Chemical oxygen demand was analysed by Hach Lange LCI400 cuvette tests with a measurement uncertainty of 10%.

The analyses were conducted in the laboratories of Povodí Moravy, s.p. (the local river basin management company), accredited under EN ISO/IEC 17025:2017. The resulting charge balance errors were at the level of $\pm 10\%$. The Geochemist's Workbench software (gwb.com 2023) was used to evaluate hydrochemical parameters. The primary assessment is based on determining N–NO₃, N–NH₄, COD, pH and EC concentrations. A total of 1147 determinations were made, and values below LOQ were replaced with $0.5 \times \text{LOQ}$. Since concentrations below the LOQ are of crucial importance in this type of assessment, they could not be excluded as they were necessary for statistical evaluation (Güler et al. 2002). All 1147 values obtained from 36 sites were assessed, including N-total, N–NO₃, N–NH₄, COD, pH and EC determinations. Nitrite anions were determined in randomly selected samples. Since their values were always less than the LOQ, their determination was omitted; the control can be carried out as a possible deviation of the sum of N–NH₄, N–NO₃ from N-total.

Sourcing remote sensing data

Remote sensing data were sourced by Sentinel 2 A, a satellite acquiring 13 different bands within a temporal resolution of 10 days. It provides a spatial resolution of 10 m for bands 2–4; 8 and 20 m for bands 5–7, 8 A, 11 and 12; and 60 m for bands 1, 9 and 10. Temporal resolution was ten days (European Space Agency – ESA, 2015). Imagery for selected bands 4 (red band) and 8 (near infrared band) were accessed through EO Browser (Sinergise Ltd. 2022) and downloaded as a raw 32-bit Tiff format. For the model area, a spring vegetation period was selected to run from 04–12–2022 to 26–06–2022 to cover the vegetation stages of the crop until the harvest (24–06–2022). Five data sourcing dates with less than 3% cloud cover were selected: 12–04–2022, 12–05–2022, 20–05–2022, 19–06–2022 and 26–06–2022.

The normalised difference vegetation index (NDVI) was calculated in QGIS (QGIS.org 2022) using a raster calculator via the standard NDVI formula ($\text{NDVI} = (\text{NIR} - \text{RED}) / (\text{NIR} + \text{Red})$) (Rouse et al. 1974). Mean values and standard deviations of taken images were calculated using the Cell Statistic tool in QGIS. NDVI images were further visualised in QGIS in a 10-class quantile classification. The NDVI

index was calculated and interpreted only in relatively large areas of homogeneously sown seasonal vegetation (crops).

Land use analysis and pedology

Historical aerial photographs from 1950 to 2021 were georeferenced and vectorised for the study area in the QGIS software environment (Geoportal 2017). The area's land use before 1950 was assessed using a historical cadastral map from 1836 (Geoportal 2017).

Historical pedology maps provided the basis for producing 1:50,000 maps in the QGIS software environment. Data sourced from pedological maps were refined through a pedological survey. Embedded pedological probes with a depth of 1 m were used for the pedological survey. The IUSS WRB (2015) world classification was used (Mantel 2023). The primary pedological classification was based on maps and documents from the 1960s, on which 1:100,000 and 1:50,000 soil maps were produced.

Results

Water analysis

Collected water samples were classified based on their chemical composition and physical parameters. Basic water types were defined and parameters typical of the groups defined in Table 1 were determined.

Group 1 – Surface and near surface water

The prevailing water type (11 out of 12) is Ca–HCO₃; pH values range from 6.2 to 9.48, with a median of 7.45. The Javorová spring (S-09) is a Ca–SO₄ type water with a median pH of 6.79; this is because the water flows exclusively in the Palaeozoic greywacke clasts. EC Group 1 values range from a minimum of 187.8 $\mu\text{S}\cdot\text{cm}^{-1}$ to a maximum of 2650 $\mu\text{S}\cdot\text{cm}^{-1}$ with a median of 605 $\mu\text{S}\cdot\text{cm}^{-1}$. The value of 2650 $\mu\text{S}\cdot\text{cm}^{-1}$ observed at site S-07 is an exceptional figure for which no association with other parameters was found; the median values were 641 $\mu\text{S}\cdot\text{cm}^{-1}$ for EC; 15.60 $\text{mg}\cdot\text{l}^{-1}$ for COD; 4.70 $\text{mg}\cdot\text{l}^{-1}$ for N–NO₃[–]; and 0.10 $\text{mg}\cdot\text{l}^{-1}$ for N–NH₄⁺. The water flows through a municipality with an unsatisfactory connection to the sewerage system.

Across Group 1, N–NO₃[–] concentrations reach a median of 4.55 $\text{mg}\cdot\text{l}^{-1}$ and range from LOQ to 20.00 $\text{mg}\cdot\text{l}^{-1}$, while N–NH₄⁺ concentrations reach a median of 0.035 $\text{mg}\cdot\text{l}^{-1}$ and range from between LOQ and 1.900 $\text{mg}\cdot\text{l}^{-1}$. COD has a median of 11.80 $\text{mg}\cdot\text{l}^{-1}$. In most instances, the concentration of N–NO₃[–] consistently exceeds that of N–NH₄⁺ ($p < 0.01$,

Wilcoxon matched-pairs signed rank test; Fig. 3a–e, Supplementary Table 2).

The rather high nitrogen concentrations in the drainage water are primarily attributed to the application of agricultural fertilisers and/or the presence of wastewater discharged from municipalities upstream of the sampling sites or both factors. Field observations make it evident that the sewage discharged often exceeds the natural volumes of the flows.

Group 2 – Groundwater

Ca–HCO₃ is the dominant water type, found in 11 of 13 boreholes. The water from borehole G-11 is classified as the Ca–SO₄ type with a median pH of 6.85. Although the borehole was drilled in limestone, the water type indicates communication (input) from Palaeozoic clasts situated southwards.

The Na–Cl water type was detected in borehole G-13 with a median electric conductivity of 2352 $\mu\text{S}\cdot\text{cm}^{-1}$, COD reaching a median of 10.20 $\text{mg}\cdot\text{l}^{-1}$. The Na–Cl type water occurs in clay layers of the filling of the Miocene age.

Outside of the water contained in borehole G-13, the EC ranges from 21.91 $\mu\text{S}\cdot\text{cm}^{-1}$ – this unusually low value is likely due to rapid infiltration of precipitation – to the maximum value of 2289 $\mu\text{S}\cdot\text{cm}^{-1}$ as observed in borehole G-09.

Throughout the group, the N–NO₃ concentrations reach a median of 4.20 $\text{mg}\cdot\text{l}^{-1}$ and range from LOQ to 13.000 $\text{mg}\cdot\text{l}^{-1}$; the N–NH₄ concentrations reach a median of 0.080 $\text{mg}\cdot\text{l}^{-1}$ and range from LOQ to 10.00 $\text{mg}\cdot\text{l}^{-1}$ ($p < 0.01$, Wilcoxon matched-pairs signed rank test; Fig. 3a–e, Supplementary Table 2).

For Borehole G-12, however, the N–NH₄ median of 6.80 exceeds the N–NO₃ median of 4.90 with a relatively high electrical conductivity of 1255 $\mu\text{S}\cdot\text{cm}^{-1}$ and, at the same time, a low pH with a median of 6.84. The borehole is located on a recently decommissioned farm site where no waste management system had been set up. Thus, contamination and elevated NH₄⁺ and Cl⁻ originated from dung water that leaked into the groundwater in an uncontrolled manner. In borehole G-12, Palaeozoic limestones are found at a depth of 1–50 m below the surface, while a water-filled karst space was discovered at a depth of 34.6–36.1 m below the surface. Here, N–NO₃⁻ contaminated karst water is present already, deep below the surface.

Group 3 – Karst water

Group 3 waters are found in caves of hypogenic origin. Primarily based on pH and EC, they can be classified as simple karst waters (Group 3a) and deep circulation system waters (Group 3b); the latter are generally considered to be hypogene karst waters. Sites in group 3b are in active contact

with CO₂ and possess elevated temperatures, corresponding to the acidic pH, high electrical conductivity and low COD values (Fig. 3a–e).

For three sites within group 3a, two are located in the ZAC. The local Cave of death has N–NO₃ levels (median: 2.6 $\text{mg}\cdot\text{l}^{-1}$) higher than levels of N–NH₄ (median: 0.02 $\text{mg}\cdot\text{l}^{-1}$); the ZAC – Nameless cave site has N–NO₃ levels (median: 0.67 $\text{mg}\cdot\text{l}^{-1}$) higher than N–NH₄ (median: 0.02 $\text{mg}\cdot\text{l}^{-1}$) levels. These caves are replenished with shallow circulation water from the Aquifer I system.

The SWCh site found in the Hranice abyss 6 m deep under the water surface has N–NO₃ levels (median: 2.20 $\text{mg}\cdot\text{l}^{-1}$) higher than levels of N–NH₄ (median 0.02 $\text{mg}\cdot\text{l}^{-1}$). Included in the Aquifer I system, this cave part is actively replenished with shallow circulation water.

For Group 3b, N–NH₄⁺ concentrations overwhelmingly exceed N–NO₃⁻ concentrations. This makes this group significantly different from Group 3a. In balneological boreholes R–II and R–III, nitrate concentrations were below the detection limit in all cases. In borehole R–I, they slightly exceeded the detection limit only once, to an N–NO₃⁻ value of 0.12 $\text{mg}\cdot\text{l}^{-1}$. In the Hranice Abyss, at the Severozápadní kanál (Northwest Channel) site at 30 m depth, N–NO₃⁻ concentrations were consistently below the LOQ; in the case of rising warm water at 30, 40 and 60 m depth, N–NO₃⁻ concentrations exceeded the LOQ level slightly only once. At the ZAC site (B point), N–NO₃⁻ concentrations slightly exceeded the LOQ on three occasions in a way that they were about twice as high as N–NH₄⁺ concentrations.

Land cover change, NDVI and representation of soils.

The spatial composition based on percentage shows a relatively stable land use matrix. From a long-term perspective, land use does not change significantly (Fig. 4). For the 1950 to 2021 period, land use can be classified under five indicators: Woody area percentage (WAP), cropland percentage (CP), Grassland percentage (GP), Water bodies' percentage (WBP) and Built-up area percentage (BAP). These indicators provide insight into the various components of the landscape and assess its overall composition.

The low NDVI in the northern area of the chasm features withered vegetation, even though the rest of the farmland cover is in a good state of health. This image shows the presence of highly permeable soils that do not retain moisture and allow high seepage of water into the underlying limestones (Fig. 5, Supplementary Fig. 7). The HA–SWCh water sampling site is the closest to this location. Thus, landscape analysis through NDVI is an effective tool for identifying areas with an extraordinary water regime.

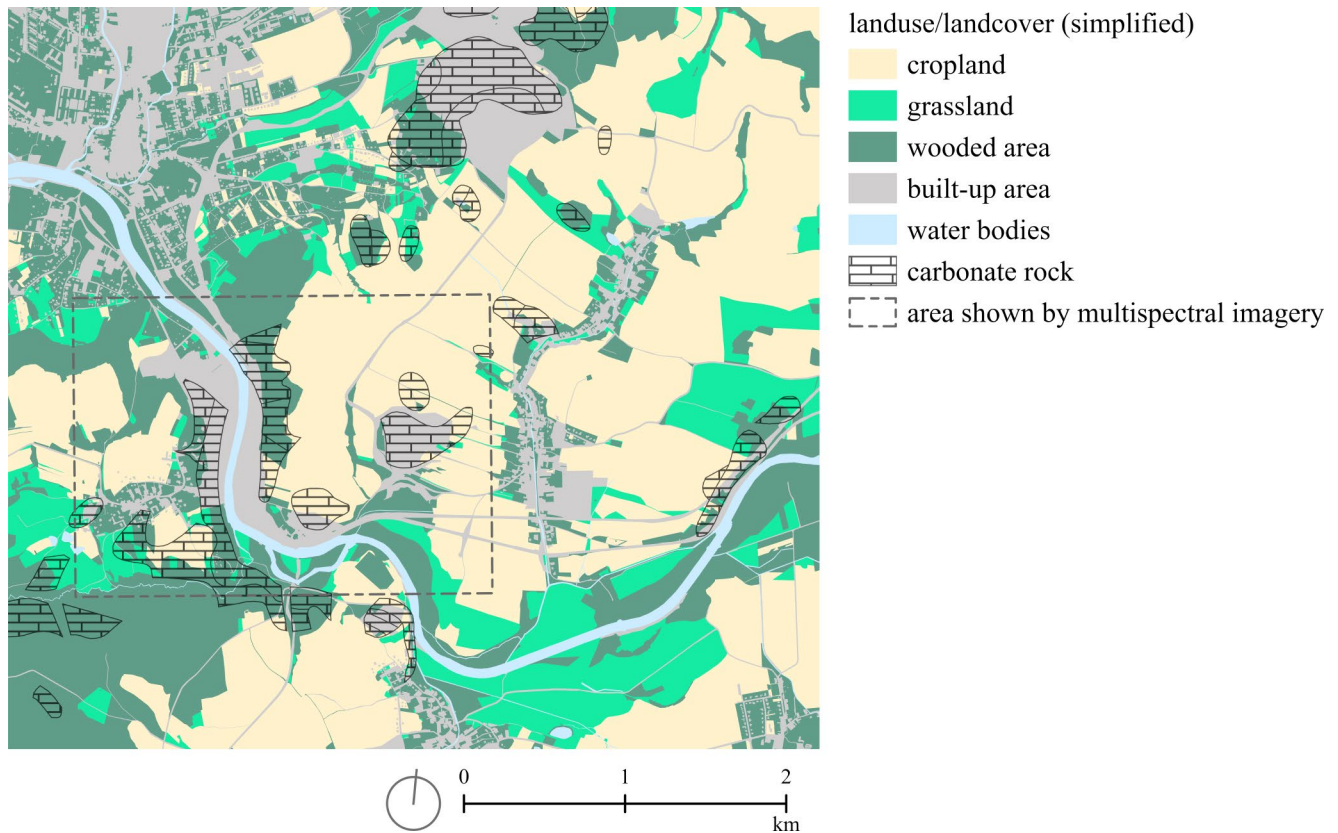
The surroundings of the Hranice abyss are formed by RSG Arenosols, which turn, towards the north, into tracts of various sizes involving Rendzic Leptosols with limestone outcrops. A layer of loess loam material of varying thickness

Table 2 Statistical parameters of water groups

N-NO3	G1	G2	G3a	G3b
n	92	57	25	71
Minimum	0.050	0.050	0.100	0.050
Q1	1.800	0.215	0.690	0.050
Median	4.550	4.200	2.300	0.050
Q3	9.375	7.000	2.750	0.050
Maximum	20.000	13.000	3.200	0.310
IQR	7.575	6.785	2.060	0.000
Mean	5.775	4.327	1.820	0.064
Std. deviation	4.887	3.893	1.052	0.046
Skewness	0.803	0.415	-0.331	4.348
Kurtosis	-0.155	-1.037	-1.559	20.233
Q1 - lower quartile; Q3 - upper quartile; IQR - interquartile range				
N-NH4	G1	G2	G3a	G3b
n	92	57	25	71
Minimum	0.010	0.010	0.010	0.070
Q1	0.013	0.040	0.020	0.140
Median	0.035	0.080	0.020	0.170
Q3	0.080	0.440	0.040	0.330
Maximum	1.900	10.000	0.100	0.500
IQR	0.068	0.400	0.020	0.190
Mean	0.079	0.911	0.034	0.226
Std. deviation	0.209	2.200	0.029	0.109
Skewness	7.608	2.948	1.665	0.558
Kurtosis	64.623	7.910	1.441	-1.005
pH	G1	G2	G3a	G3b
n	91	54	19	64
Minimum	6.200	6.160	6.130	5.900
Q1	6.950	6.833	6.270	6.020
Median	7.450	7.025	6.440	6.085
Q3	7.790	7.330	6.520	6.258
Maximum	9.480	9.890	7.060	6.480
IQR	0.840	0.498	0.250	0.238
Mean	7.406	7.221	6.446	6.136
Std. deviation	0.591	0.729	0.233	0.145
Skewness	0.418	2.399	1.001	0.483
Kurtosis	0.566	6.309	1.467	-0.866
EC	G1	G2	G3a	G3b
n	91	54	20	64
Minimum	187.800	21.910	1247.000	2121.000
Q1	429.000	631.250	1417.250	2254.000
Median	605.000	826.500	1499.500	2355.000
Q3	692.000	1326.500	1678.500	2642.500
Maximum	2650.000	2573.000	2140.000	2820.000
IQR	263.000	695.250	261.250	388.500
Mean	600.533	1021.063	1537.500	2438.328
Std. deviation	301.551	549.482	221.539	210.206
Skewness	3.630	1.099	1.044	0.264
Kurtosis	23.375	1.094	1.694	-1.477
COD	G1	G2	G3a	G3b
n	89	48	14	49
Minimum	1.700	0.250	0.210	0.111
Q1	7.695	6.625	0.438	0.303
Median	11.800	10.200	1.590	0.706
Q3	18.350	14.675	2.240	1.515
Maximum	63.500	56.100	6.700	15.600

Table 2 (continued)

IQR	10.655	8.050	1.803	1.212
Mean	16.084	11.557	1.749	1.595
Std. deviation	13.644	9.119	1.667	2.665
Skewness	1.913	2.728	2.150	3.814
Kurtosis	3.379	11.620	6.026	16.892

**Fig. 4** Land Use / Land cover of the surrounding landscape and delimitation of the carbonate rocks

often covers the limestones. The upper parts of the Hranice abyss consist of Miocene sandstones, so the soils of the immediate forested surroundings of the abyss are members of RSG Arenosols (Supplementary Fig. 8). The RSG Arenosols extend as far as several dozen metres into the agriculturally used land that forms the eastern edge of the chasm. They are mixed with a heavier soil-forming substrate on arable land – loess loam. The loess substrate was deposited here due to the eolic activity of the late glacial period. Agriculturally used soil other than that mentioned above is mainly composed of members of RSG Haplic Luvisols in various stages of erosion or accumulation, which in several places turn into Colluvic Regosols. In shallow soils on the Miocene sandstone outcrops, members of RSG Leptosols can also be found towards the south.

Discussion

Land use analyses in relation to nitrogen distribution

Karst aquifers possess distinct hydraulic and hydrogeological attributes that render them highly susceptible to pollution resulting from human activities. The structure of karst aquifers is distinguished by both rapid conduits and slower pathways, such as fractures and sediments, through which water flows, enabling both laminar and turbulent flows. A study by Ulloa-Cedamano et al. (2022) found a strong correlation between changes in landscape structure and stream hydrochemistry. Land use and land cover modification challenge the hydrologic system sustainability – not only by the overall composition but also by the intensity of agricultural activity. Based on the assessment of the long-term development of land use in the Hranice Karst and its surroundings,

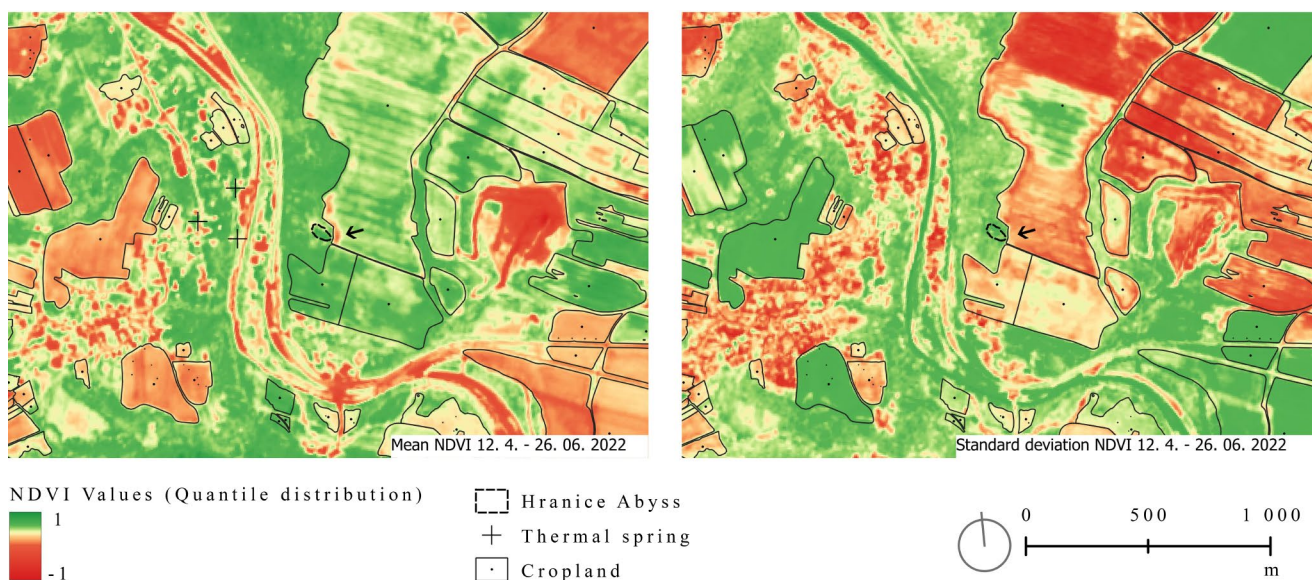


Fig. 5 NDVI changes in the vicinity of Hranice Abyss and mineral springs. The arrow points to highly permeable soils in the northern vicinity of the abyss and possible seepage of water into the limestone bedrock

we found that no major changes occurred there in terms of land use. Larger agricultural plots allow more intense agricultural techniques and fewer subtle farming practices. Even partial deforestation and agricultural use of the landscape interrupt the original state of nutrient recycling. The intensity of land cultivation, the use of fertilisers and, eventually, the increasing intensity of urbanisation, all certainly have an impact on these processes; however, they cannot be assessed through land-use change assessments very well. Usually, the nutrients released by decomposers from the decomposed biomass are re-used to a large extent, but this only happens to a limited extent in a system with a fast turnover of nutrients. Such systems are thus dependent on additional inputs, and excess nutrients are, on the contrary, leached into subsurface waters. In addition, as alteration of the evapotranspiration current increases the amount of water flowing through the soil, there is increased leaching of the soil and of the soil-forming substrate. The Normalised Difference Vegetation Index (NDVI) is one of the most frequently used indices for determining vegetation vitality and biomass volume (Rouse et al. 1974). NDVI combines near-infrared radiation and red radiation to delineate vegetation in stress or different phenostages. Normalised difference vegetation indices typically range from 0.1 up to 0.9, with higher values associated with greater density and greenness of the plant canopy. Soil values are close to zero. When plants are subjected to pressure due to water, diseases or other environmental factors, plant leaves reflect significantly less NIR and more red irradiance. As a result, the NDVI value is smaller than usual when plants are subjected to stress (Lillesand et al. 2015). The spatial analysis of NDVI revealed a possible infiltration site near the Hranice

abyss (Fig. 5). The NDVI is not directly linked to groundwater quality, yet it can provide information about potential changes in water availability and vegetation health. In some instances, NDVI changes can indicate a decline in vegetation health and, in turn, suggest changes in the availability or quality of groundwater. These waters are enriched with nitrogen; they occur as drainage waters in other parts of the territory. Long underground channels bring water into the Hranice abyss area. Therefore, the nitrogen-enriched waters from agricultural runoff are the suspected source of nitrogen pollution within the studied hypogene karst environment. However, they can only get deeper underground in places where the permeable rock is made up of, for example, sandstone, which forms the overburden of the karst environment.

Nitrogen cycle in hypogene karst

Nitrate nitrogen values detected in the groundwater of the Hranice Karst – including wells and caves were not exceeding a maximum of 3.2 mg.l^{-1} . This value is not extreme when compared to the results found in the Moravian Karst drip water where nitrate nitrogen reached 46.8 mg.l^{-1} (Chalupka 2022). The Hranice Karst is an agriculturally exploited area featuring drainage systems (Supplementary Fig. 3). In recent studies worldwide, drainage systems were identified as a significant source of agricultural pollution, especially nitrate-nitrogen (Fučík et al. 2017; Kulhavý et al. 2007), pesticides (Zajíček et al. 2018; Brown and van Beinum 2009) and pesticide metabolites, and soluble forms of phosphorus (Zajíček et al. 2022).

Water discharged from municipal wastewater treatment plants into streams represents the majority of water

especially during hot summer periods in the Hranice area. Due to these conditions, the rock composition of the stream channel is crucial. In cases when it is formed by impermeable clays, the water flows into the River Bečva. However, where the bedrock is formed by karst rock part of the water is drained vertically leading to direct input of contaminated water into the karst environment. A specific situation occurs where the bedrock consists of Neogene and Quaternary clayey sediments surrounded with rather coarse fluvial sediments in the floodplain (Supplementary Fig. 9).

The time required for nitrogen to be transported through the soil and rock environment from the source (e.g., the area of fertiliser application) to the recipient (the water body or the sampling point), represents a critical value in the process of pollutant displacement. The groundwater residence times of 17–50 years were suggested for the Hranice area (Švajner 1982; Maník et al. 1992; Sracek et al. 2019). The biogeochemical time delay is essential in understanding nitrogen dynamics and the potential impacts of the element on water quality (Huebsch et al. 2013; Sousa et al. 2013; Baily et al. 2011).

This wide time range probably reflects the variability caused by the presence of differently permeable bedrock. The presence of the impermeable Neogene clays certainly leads to a primary slow-down infiltration. Conversely, in areas with sandstones, increased infiltration is proved by NDVI.

As nitrogen is the only water contaminant found in the immediate vicinity, it is evident from the results that ammoniacal nitrogen is not the primary form of nitrogen found in the water and does not signal any acute pollution (Fig. 3d, e and a–e, Supplementary Table 2). Anoxic and reducing conditions in the groundwater (deep wells) prevent the nitrification of NH_4^+ through the Dissimilatory Nitrate Reduction to Ammonium (DNRA) process. The importance of DNRA is usually subordinate to denitrification (Simon and Klotz 2013; Appelo and Postma 2004; Smith et al. 1991), but in some climates, especially warm and humid, DNRA may be essential as a process (Rütting et al. 2011). The high ammonium concentrations observed in the deep wells within karst aquifers system II, especially those considered to be hypogene, suggest that DNRA could be actively occurring in these environments. The anoxic conditions caused with excess CO_2 are typical feature of the Hranice aquifers. The anoxia lead to inhibition of nitrification and promote DNRA thus the accumulation of ammonium in deep environment can be expected. This is contrary to the expectation that ammonium, if sourced from surface pollution, would be more prevalent in shallower boreholes. The suggested mechanism explains ammonium presence in the unique deep hypogene karst environment. The presence of nitrate reduction-associated bacteria, such as *Pseudomonas*,

Burkholderiales, and *Rhizobiales*, in the Hranice Abyss, as identified in earlier studies (e.g. Pavlík et al., 2018) supports the atypical nitrogen cycle. Their presence in the Hranice Abyss supports the notion that microbial processes may significantly contribute to the nitrogen dynamics within the deep wells, particularly influencing the ammonia concentration in waters of hypogene origin. The high ammonia content in the water originating from HA can be explained based on the presence of electron donors and their role in the local water chemistry. In the case of NH_4^+ in the groundwater of the Hranice Karst, including wells and caves, the highest recorded value was 9.4 mg.l^{-1} , while in 2021, in other karst regions of the Czech Republic, concentrations ranged from 0.02 to 0.04 mg.l^{-1} (Chalupka 2022). Given the suitable conditions of warmth and low oxygen availability in the deep groundwater, denitrification can remove nitrates from the system to a significant degree (Fig. 3a–e, Supplementary Table 2). Denitrification depletes nitrates in geothermal water (Wu et al. 2020).

Biogenic materials have accumulated via the opening of the abyss. The dry cave area, known as Rotunda, houses a substantial population of *Myotis myotis* bats, whose guano accounts for the organic matter in the cave (Pavlík et al. 2018; Vysoká et al. 2019). Biomass falling into the abyss as plant residues cannot be a significant source of N. In ZAC I, the balneological borehole environment is maintained clean, yet N-NH_4^+ concentrations are higher. Water samples taken from the warm waters emerging in the abyss that are free of biomass show elevated N-NH_4^+ concentrations as well.

Based on the form of N present, the karst waters were subdivided into two groups. Group I is characterised by a decrease in the NO_3^- content and an increase in NH_4^+ cations. All waters are gaseous hydrothermal mineral waters, with a high content of CO_2 exhibiting similarities to balneological wells (R–I, R–II and R–III) and the NO_3^- is released into anoxic environments. Group II includes waters located in the karst environment with more N-NO_3^- compared to N-NH_4^+ . This occurs when the rapid water infiltration takes place directly in the karst environment and NO_3^- does not have enough time to be converted to NH_4^+ . It can be assumed that the above ammonia–nitrate–nitrogen relationships have prevailed at the study sites for a long time. The above facts indicate that no fundamental contradiction would invalidate the hypothesis that the sampled waters are located at sites where further infiltration can occur, thus becoming part of Hranice Karst mineral waters.

Despite the high vulnerability of karst aquifers to water quality issues, exploration, understanding and interpretation of the systems remain challenging, primarily due to the unique groundwater flow patterns within the conduit systems (Göppert and Goldscheider 2008; Ravbar and Goldscheider 2007). In some areas, it is not reasonably possible to

determine places where tracers would be possible to apply or collect (e.g. Sracek et al. 2019).

The described process of N-NO_3^- to N-NH_4^+ transformation, together with the assessment of changes in NDVI and geological structure, can thus contribute to the identification of places where surface water infiltrates and, subsequently, generates karst mineral waters.

Conclusion

The present study documented, through systematic monitoring of watercourses, that the discharge of wastewater into low-watery or occasional streams needs detail monitoring and evaluation. The behaviour of the nitrogen in the Hranice hypogene Karst is the result of heterogenous geological structure and influx of CO_2 to the area. The observed features are thus masked and their identification was possible only using multiapproach combining NVDI and analytical geochemistry. The land use analysis enabled the identification of places where permeable strata are present and contamination can enter the sensitive karst system. Using satellite imaging and normalised difference vegetation index (NDVI) analysis, areas with debilitated vegetation were found. A pedological survey verified that these areas have been formed from highly permeable sandstones of the Miocene age.

A direct correlation was found between the occurrence of karst waters with a high CO_2 content and the form of N. The results obtained proved that nitrogen NO_3^- compounds are converted into NH_4^+ compounds in an anoxic environment. It was also proved that the NH_4^+ present in karst thermal waters comes from agricultural activity on the surface. These permeable layers are overlying karst carbonate rocks and serve as conduits for contaminants. The water analyses, landscape use, remote sensing of the Earth and pedological survey, all proved to be essential tools for identifying the origin of pollution in the karst waters.

Supplementary Information The online version contains supplementary material available at <https://doi.org/10.1007/s12665-024-11936-0>.

Acknowledgements The Gregor Johann Mendel Grant Agency of the Mendel University in Brno financially supported the research as part of the project entitled Landscape in Whole and Landscape in Detail – an Interdisciplinary Research of the Hranice Karst. The authors greatly appreciate Michal Guba, Martin Strnad, Vlastimil Zela, Miroslav Lukáš, Petr Hřebejk, Pavel Fryšák, Jan Musil, Martin Prachař, Zbyněk Sedlák and other cave divers, members of the Czech Speleological Society for underwater sampling, as well as the staff, above all Barbora Šimečková and Slavomír Černý of the Cave Authority of the Czech Republic, Zbrašov Aragonite Caves headquarters. We thank Povodí Morava s.p. for allowing access to the sampling sites.

Author contributions M.G. wrote the main manuscript text. J.S., O.U., K.K., R.K. prepared GIS processing. M.G., P.O., O.U. prepared water analysis. V.V. prepared pedological studies. V.B., M.G. prepared the statistical analysis. All authors read and approved the final manuscript.

Funding Open access publishing supported by the National Technical Library in Prague.

Data availability No datasets were generated or analysed during the current study.

Declarations

Competing interests The authors declare no competing interests.

Open Access This article is licensed under a Creative Commons Attribution 4.0 International License, which permits use, sharing, adaptation, distribution and reproduction in any medium or format, as long as you give appropriate credit to the original author(s) and the source, provide a link to the Creative Commons licence, and indicate if changes were made. The images or other third party material in this article are included in the article's Creative Commons licence, unless indicated otherwise in a credit line to the material. If material is not included in the article's Creative Commons licence and your intended use is not permitted by statutory regulation or exceeds the permitted use, you will need to obtain permission directly from the copyright holder. To view a copy of this licence, visit <http://creativecommons.org/licenses/by/4.0/>.

References

- Appelo CAJ, Postma D (2004) Geochemistry, groundwater and pollution. CRC. <https://doi.org/10.1201/9781439833544>
- Baily A, Rock L, Watson CJ, Fenton O (2011) Spatial and temporal variations in groundwater nitrate at an intensive dairy farm in south-east Ireland: Insights from stable isotope data. *Agric Ecosyst Environ* 144(1):308–318. <https://doi.org/10.1016/j.agee.2011.09.007>
- Barry JD, Runkel AC, Calvin Alexander E (2023) Synthesizing multifaceted characterization techniques to refine a conceptual model of groundwater sources to springs in valley settings (Minnesota, USA). *Hydrogeol J* 31:707–729. <https://doi.org/10.1007/s10040-023-02613-w>
- Bosák P (2000) Notes on the history of some karstological terms – hydrothermal karst, geysermite, vadose zone. *Acta carsologica* 29(2):233–240
- Bouraoui F, Grizzetti B (2014) Modelling mitigation options to reduce diffuse nitrogen water pollution from agriculture. *Sci Total Environ* 468:1267–1277. <https://doi.org/10.1016/j.scitotenv.2013.07.066>
- Brown C, Van Beinum W (2009) Pesticide transport via sub-surface drains in Europe. *Environ Pollut* 157:3314–3324. <https://doi.org/10.1016/j.envpol.2009.06.029>
- Buvaneshwari S, Riotte J, Sekhar M, Mohan Kumar MS, Sharma AK, Duprey JL, Audry S, Giriraja PR, Praveenkumarreddy Y, Hemanth M, Durand P, Braun JJ, Ruiz L (2017) Groundwater resource vulnerability and spatial variability of nitrate contamination: Insights from high-density tubewell monitoring in a hard rock aquifer. *Sci Total Environ* 579:838–847. <https://doi.org/10.1016/j.scitotenv.2016.11.017>

- Cháb J (2010) Outline of the geology of the Bohemian Massif: the basement rocks and their Carboniferous and Permian cover. Czech Geological Survey, Prague
- Chalupka F (2022) Kvalita podzemních vod chráněných území ČR. Jsme na tom špatně? In: Baldík V (ed) Sborník referátů 1. ročníku konference Kras, jeskyně a lidé. Acta Speleologica. (In Czech)
- Chen YP, Chen SQ, Yu JJ, Wen XW, Xu JJ (2024) Evaluation on the effect of water environment treatment – A new exploration considering time based on the RCS. Applied Intelligence 54, 5 (Mar 2024), 4277–4299. <https://doi.org/10.1007/s10489-023-05218-8>
- Coxon C (2011) Agriculture and karst. In: van Beynen P (ed) Karst Management. Springer, Dordrecht, pp 103–138. https://doi.org/10.1007/978-94-007-1207-2_5
- Cui S, Shi Y, Groffman PM, Schlesinger WH, Zhu YG (2013) Centennial-scale analysis of the creation and fate of reactive nitrogen in China (1910–2010) Proceedings of the National Academy of Sciences, 2013. 110(6):2052–2057. <https://doi.org/10.1073/pnas.1221638110>
- Dlešťík P, Bábek O (2013) Shallow geophysical mapping of buried karst surface near Hranice using electrical resistivity tomography. Geol výzkumy na Moravě ve Slezsku 20(1–2):174–177 (In Czech). <https://journals.muni.cz/gvms/article/view/1568/1205>
- EN ISO/IEC 17025:2017 General requirements for the competence of testing and calibration laboratories
- Ford D, Williams PD (2007) Karst hydrogeology and geomorphology. John Wiley & Sons Ltd. <https://doi.org/10.1002/9781118684986>
- Fučík P, Zajíček A, Kaplická M, Duffková R, Peterková J, Maxová J, Takáčová Š (2017) Incorporating rainfall-runoff events into nitrate-nitrogen and phosphorus load assessments for small tile-drained catchments. Water 9(9):712. <https://doi.org/10.3390/w9090712>
- Geoportál Č Geoportál ČÚŽK access to map products and services of the resort. <http://geoportál.cuzk.cz>
- Geršl M (2009) Hranický kras. In: Hromas J (ed) Jeskyně ČR. Chráněná území ČR, vol 15. Agentura ochrany přírody a krajiny ČR & EkoCentrum Brno. Prague. (In Czech)
- Göppert N, Goldscheider N (2008) Solute and colloid transport in karst conduits under low- and high-flow conditions. Groundwater 46(1):61–68. <https://doi.org/10.1111/j.1745-6584.2007.00373.x>
- Güler C, Thyne GD, McCray J, Turner AK (2002) Evaluation of graphical and multivariate statistical methods for classification of water chemistry data. Hydrogeol J 10:455–474. <https://doi.org/10.1007/s10040-002-0196-6>
- Hao Z, Gao Y, Yang Y, Zhang Q (2023) Determining nitrogen fate by hydrological pathways and impact on carbonate weathering in an agricultural karst watershed. Int Soil Water Conserv Res 11(2):327–338. <https://doi.org/10.1016/j.iswcr.2022.04.002>
- Hladil J, Bosák P, Slavík L, Carew LJ, Mylroie JE, Geršl M (2003) A pragmatic test of the early origin and fixation of gamma-ray spectrometric (U, Th) and magneto-susceptibility (Fe) patterns related to sedimentary cycle boundaries in pure platform limestones. Carbonate Evaporites 18(2):89–107
- Holcová K, Hrabovský J, Nehyba S, Hladilová Š, Doláková N, Demény A (2015) The Langhian (Middle Badenian) carbonate production event in the Moravian part of the Carpathian Fore-deep (central Paratethys): A multiproxy record. Facies 61(1):419. <https://doi.org/10.1007/s10347-014-0419-z>
- Huebsch M, Horan B, Blum P, Richards KG, Grant J, Fenton O (2013) Impact of local weather conditions and agronomic practices on groundwater nitrogen content in a karst aquifer on an intensive dairy farm in Southern Ireland. Agric Ecosyst Environ 179:187–199. <https://doi.org/10.1016/j.agee.2013.08.021>
- Jiang GH, Guo F, Polk SJ, Kang ZQ, Wu JC (2015) Delineating vulnerability of karst aquifers using hydrochemical tracers in South-western China. Environ Earth Sci 74:1015–1027. DOI10.1007/s12665-014-3862-9
- Jirman P, Geršlová E, Kalvoda J, Melichar R (2018) 2d basin modelling in the eastern Variscan fold belt (Czech Republic): influence of thrusting on patterns of thermal maturation. J Pet Geol 41(2):175–188. <https://doi.org/10.1111/jpgp.12699>
- Kalvāns A, Popovs K, Priede A, Koit O, Retiķe I, Bikše J, Dēliņa A, Babre A (2021) Nitrate vulnerability of karst aquifers and associated groundwater-dependent ecosystems in the Baltic region. Environ Earth Sci 80:628. <https://doi.org/10.1007/s12665-021-09918-7>
- Klanica R, Kadlec J, Tábořík P, Mrlina J, Valenta J, Kováčiková S (2020) Hypogenic versus epigenic origin of deep underwater caves illustrated by the Hranice Abyss (Czech Republic)—The world's deepest freshwater cave. J Geophys Research: Earth Surf 125(9):e2020JF005663. <https://doi.org/10.1029/2020JF005663>
- Klimchouk A, Palmer AN, de Waele J, Auler AS, Audra P (2017) Hypogenic karst regions and caves of the world. Springer International Publishing, New York. <https://doi.org/10.1007/978-3-319-53348-3>
- Kulhavý Z, Doležal F, Fučík P, Kulhavý F, Kvítek T, Muzikář R, Soukup M, Švihla V (2007) Management of agricultural drainage systems in the Czech Republic. Irrig Sci 56(S1):S141–S149. <https://doi.org/10.1002/ird.339>
- Li J, Zou S, Wang J, Zhou C, Wu Y, Zhang H, Zhao Y, Yang G (2023) Spatiotemporal variability and control factors of NO₃⁻ in a polluted karst water system of an agricultural wetland in South China. Chemosphere 313:137435. <https://doi.org/10.1016/j.chemosphere.2022.137435>
- Lillesand T, Kiefer RW, Chipman J (2015) Remote Sensing and Image Interpretation. Wiley
- Liu L, Bian Z, Ding S (2020) Consequences of spatial heterogeneity of forest landscape on ecosystem water conservation service in the Yi River Watershed in Central China. Sustainability 12(3):1170. <https://doi.org/10.3390/su12031170>
- Lorette G, Peyraube N, Lastennet R, Denis A, Sabidussi J, Fournier M, Viennet D, Gonand J, Villanueva JD (2020) Tracing water perturbation using NO₃⁻, doc, particles size determination, and bacteria: A method development for karst aquifer water quality hazard assessment. Sci Total Environ 725:138512. <https://doi.org/10.1016/j.scitotenv.2020.138512>
- Lorette G, Sebilo M, Buquet D, Lastennet R, Denis A, Peyraube N, Charriere V, Studer JC (2022) Tracing sources and fate of nitrate in multilayered karstic hydrogeological catchments using natural stable isotopic composition (δ¹⁵N-NO₃⁻ and δ¹⁸O-NO₃⁻). Application to the Toulon karst system (Dordogne, France). J Hydrol 610:127972. <https://doi.org/10.1016/j.jhydrol.2022.127972>
- Maník R, Michalíček M, Procházková V (1992) Geochemistry of selected natural healing and table mineral waters of the Czech Republic – verification stage. MS Geofond P84572, Czech Geological Survey. (In Czech)
- Mantel S, Dondeyne S, Deckers S (2023) World reference base for soil resources (WRB). Reference Module in Earth Systems and Environmental Sciences. Elsevier, Amsterdam, p 9780128229743002000
- Maurya PK, Ali SA, Zaidi SK, Wasi S, Tabrez S, Malav LC, Ditthakit P, Son CT, Cabral-Pinto MMS, Yadav KK (2023) Assessment of groundwater geochemistry for drinking and irrigation suitability in Jaunpur district of Uttar Pradesh using GIS-based statistical inference. Environ Sci Pollut Res 30:29407–29431. <https://doi.org/10.1007/s11356-022-23959-w>
- Meyberg M, Rinne B (1995) Messung des ³He/⁴He-Isotopenverhältnisses im Hranicka Propast (Tschechische Republik). Die Höhle, Zeitschrift für Karst- und Höhlenkunde. 46(1):5–8
- Nietch CT, Hawley RJ, Safwat A, Christensen JR, Heberling MT, McManus J, McClatchey R, Lubbers H, Smucker NJ, Onderak E, Macy S (2024) Implementing constructed wetlands for nutrient reduction at watershed scale: Opportunity to link models and

- real-world execution. *Journal of Soil and Water Conservation* May 2024, 79 (3) 113–131; <https://doi.org/10.2489/jswc.2024.00077>
- Otava J, Geršl M, Havří J, Bábek O, Kosina M (2009) The Hranice Abyss—Through the eyes of geologists. *Ochrana přírody* 64(1):18–22 (In Czech)
- Pavlik I, Geršl M, Bartos M, Ulmann V, Kauccka P, Čaha J, Unc A, Hubelova D, Konecny O, Modra H (2018) Nontuberculous mycobacteria in the environment of Hranice Abyss the world's deepest flooded cave (Hranice karst, Czech Republic). *Environ Sci Pollut Res* 25:23712–23724. <https://doi.org/10.1007/s11356-018-2450-z>
- Qiu J, Turner MG (2015) Importance of landscape heterogeneity in sustaining hydrologic ecosystem services in an agricultural watershed. *Ecosphere* 6(11):1–19. <https://doi.org/10.1890/ES15-00312.1>
- Quitt E (1971) Climatic regions of Czechoslovakia. Brno. Geografický ústav ČSAV. (In Czech)
- Quitt E (1975) Map of Czechoslovak climatic regions 1: 500 000. Geografický ústav ČSAV, Brno. (In Czech)
- Ravbar N, Goldscheider N (2007) Proposed methodology of Vulnerability and Contamination Risk Mapping for the Protection of Karst Aquifers in Slovenia. *Acta carsologica* 36(3). <https://doi.org/10.3986/ac.v36i3.174>
- Ravbar N, Petrič M, Blatnik M, Švara A (2021) A multi-methodological approach to create improved indicators for the adequate karst water source protection. *Ecol Ind* 126:107693. <https://doi.org/10.1016/j.ecolind.2021.107693>
- Řezníček V (1977) Hydrogeological study Teplice n. Bečvou – drinking water, MS Geofond P87500. (In Czech)
- Rouse JW, Haas RH, Schell JA, Deering DW (1974) Monitoring Vegetation Systems in the Great Plains with ERTS. Third ERTS-1 Symp NASA NASA SP-351:309–317 Washington DC
- Rütting T, Huygens D, Staelens J, Müller C, Boeckx P (2011) Advances in 15 N-tracing experiments: new labelling and data analysis approaches. *Biochem Soc Trans* Jan 39(1):279–283. <http://doi.org/10.1042/BST0390279>
- Schulmann K, Gayer R (2000) A model for a continental accretionary wedge developed by oblique collision: the NE Bohemian Massif. *J Geol Soc Lond* 157:401–416. <https://doi.org/10.1144/jgs.157.2.401>
- Shelar RS, Nandgude SB, Pande CB, Costache R, El-Hiti GA, Tolche AD, Son CT, Yadav KK (2023) Unlocking the hidden potential: groundwater zone mapping using AHP, remote sensing and GIS techniques. *Geomatics Nat Hazards Risk* 14(1). <https://doi.org/10.1080/19475705.2023.2264458>
- Simon J, Klotz MG (2013) Diversity and evolution of bioenergetic systems involved in microbial nitrogen compound transformations. *Biochim et Biophys Acta (BBA)-Bioenergetics* 1827(2):114–135. <https://doi.org/10.1016/j.bbabi.2012.07.005>
- Sivelle V, Jourde H, Bittner D, Richieri B, Labat D, Hartmann A, Chiozna G (2022) Considering land cover and land use (LCLU) in lumped parameter modeling in forest dominated karst catchments. *J Hydrol* 612:128264. <https://doi.org/10.1016/j.jhydrol.2022.128264>
- Šmejkal V, Hladíková J, Pfeiferová A, Melková J (1974) Isotopic composition of carbon and oxygen in speleothems from karst caves in Northern Moravia. In: Proceedings of International Symposium on Water-Rock Interaction, Czechoslovakia. In: Čadek J, Pačes T (Eds.), Proceedings of International Symposium on Water-Rock Interaction, Czechoslovakia 363–367
- Smith RL, Howes BL, Duff JH (1991) Denitrification in nitrate-contaminated groundwater: Occurrence in steep vertical geochemical gradients. *Geochim Cosmochim Acta* 55(7):1815–1825. [https://doi.org/10.1016/0016-7037\(91\)90026-2](https://doi.org/10.1016/0016-7037(91)90026-2)
- Sousa T, Ingle B, Sousa S, Bhosle S (2013) Seasonal variations of nitrate reducing and denitrifying bacteria utilizing hexadecane in Mandovi estuary, Goa, West Coast of India. *Indian J Geo-Mar Sci* 42(5):587–592
- Sracek O, Geršl M, Faimon J, Bábek O (2019) The geochemistry and origin of fluids in the carbonate structure of the Hranice Karst with the world's deepest flooded cave of the Hranicka Abyss, Czech Republic. *Appl Geochem* 100:203–212. <https://doi.org/10.1016/j.apgeochem.2018.11.013>
- Švajner L (1982) Hydrogeology of mineral waters in Teplice nad Bečvou. 1982, Diploma Thesis, University of Komenský, Bratislava, Slovakia
- Tolasz R (2007) Climate atlas of Czechia. Czech hydrometeorological Institute, Prague
- Tyráček J (1962) Fossil cockpit karst near Hranice na Moravě. *Časopis pro Mineral Geol* 2:176–185 (In Czech)
- Ulloa-Cedamano F, Probst JL, Marais-Sicre C, Vrech E, Maire E, Probst A (2022) Potential influence of landscape transition on stream water chemistry trends during the last decades in a karst catchment (Pyrenees, SW France) in a context of global environmental changes. *Ecol Ind* 2022(140):109023. <https://doi.org/10.1016/j.ecolind.2022.109023>
- Van Meter KJ, Basu NB, Veenstra JJ, Burras CL (2016) The nitrogen legacy: emerging evidence of nitrogen accumulation in anthropogenic landscapes. *Environ Res Lett* 11:035014. <https://doi.org/10.1088/1748-9326/11/3/035014>
- Van Meter KJ, Basu NB, Van Cappellen P (2017) Two centuries of nitrogen dynamics: Legacy sources and sinks in the Mississippi and Susquehanna River Basins. *Glob Biogeochem Cycles* 31(1):2–23. <https://doi.org/10.1002/2016GB005498>
- Vilhar U, Kermavnar J, Kozamernik E, Petrič M, Ravbar N (2022) The effects of large-scale forest disturbances on hydrology—An overview with special emphasis on karst aquifer systems. *Earth Sci Rev* 235:104243. <https://doi.org/10.1016/j.earscirev.2022.104243>
- Vysoká H (2016) Hydrogeological survey of Hranice Abyss. Report for Expedition Neuron project, in Neuron Fund. MS, Praha, p 265
- Vysoká H, Bruthans J, Falteisek L, Žák K, Rukavičková L, Holeček J, Schweigstillová J, Oster H (2019) Hydrogeology of the deepest underwater cave in the world: Hranice Abyss, Czechia. *Hydrogeol J* 27(7):2325–2345. <https://doi.org/10.1007/s10040-019-01999-w>
- White P, Ruble CL, Lane ME (2013) The effect of changes in land use on nitrate concentration in water supply wells in southern Chester County. *Pa Environ Monit Assess* 185(1):643–651. <https://doi.org/10.1007/s10661-012-2581-5>
- Wu XC, Li CS, Sun B, Geng FQ, Gao S, Lv MH, Ma XY, Li H, Xing LT (2020) Groundwater hydrogeochemical formation and evolution in a karst aquifer system affected by anthropogenic impacts. *Environ Geochem Health* 42:2609–2626. <https://doi.org/10.1007/s10653-019-00450-z>
- Yadav KK, Gupta N, Kumar V, Choudhary P, Khan SA (2018) GIS-based evaluation of ground water geochemistry and statistical determination of the fate of contaminants in shallow aquifers from different functional areas of Agra city, India: levels and spatial distributions. *RSC Adv* 8:15876–15889. <https://doi.org/10.1039/c8ra00577j>
- Zajíček A, Fučík P, Kaplická M, Liška M, Maxová J, Dobiáš J (2018) Pesticide leaching by agricultural drainage in sloping, mid-textured soil conditions – the role of runoff components. *Water Sci Technol* 77(7–8):1879–1890. <https://doi.org/10.2166/wst.2018.068>
- Zajíček A, Hejduk T, Sychra L, Vybíral T, Fučík P (2022) How to Select a Location and a Design of Measures on Land Drainage – A Case Study from the Czech Republic. *J Ecol Eng* 23(4):43–57. <https://doi.org/10.12911/22998993/146270>
- Zhang X, Davidson EA, Mauzerall DL, Searchinger TD, Dumas P, Shen Y (2015) Managing nitrogen for sustainable development. *Nature* 528(7580):51–59. <https://doi.org/10.1038/nature15743>

Zhang Q, Qian H, Xu P, Li W, Feng W, Liu R (2021) Effect of hydrogeological conditions on groundwater nitrate pollution and human health risk assessment of nitrate in Jiaokou Irrigation District. <https://doi.org/10.1016/j.jclepro.2021.126783>. J Clean Prod

Publisher's note Springer Nature remains neutral with regard to jurisdictional claims in published maps and institutional affiliations.